Geosci. Model Dev. Discuss., 5, 4187–4232, 2012
www.geosci-model-dev-discuss.net/5/4187/2012/
doi:10.5194/gmdd-5-4187-2012

Geoscientific Model Development Discussions

Improving the representation of secondary organic aerosol (SOA) in the MOZART-4 global chemical transport model

A. Mahmud and K. C. Barsanti

Department of Civil and Environmental Engineering, Portland State University, P.O. Box 751-CEE, Portland, OR 97207–0751, USA

Received: 29 October 2012 – Accepted: 28 November 2012 – Published: 11 December 2012

Correspondence to: A. Mahmud (amahmud@pdx.edu)

Published by Copernicus Publications on behalf of the European Geosciences Union.

Abstract

The secondary organic aerosol (SOA) module in the Model for Ozone and Related chemical Tracers, version 4 (MOZART-4) has been updated by replacing existing two-product (2p) parameters with those obtained from two-product volatility basis set (2p-VBS) fits, and by treating SOA formation from the following volatile organic compounds (VOCs): isoprene, propene and lumped alkenes. Strong seasonal and spatial variations in global SOA distributions were demonstrated, with significant differences in the predicted concentrations between the base-case and updated model versions. The base-case MOZART-4 predicted annual average SOA of $0.36 \pm 0.50\,\mu g\,m^{-3}$ in South America, $0.31 \pm 0.38\,\mu g\,m^{-3}$ in Indonesia, $0.09 \pm 0.05\,\mu g\,m^{-3}$ in the USA, and $0.12 \pm 0.07\,\mu g\,m^{-3}$ in Europe. Concentrations from the updated versions of the model showed a marked increase in annual average SOA. Using the updated set of parameters alone (MZ4-v1) increased annual average SOA by ~8 %, ~16 %, ~56 %, and ~108 % from the base-case in South America, Indonesia, USA, and Europe, respectively. Treatment of additional parent VOCs (MZ4-v2) resulted in an even more dramatic increase of ~178–406 % in annual average SOA for these regions over the base-case. The increases in predicted SOA concentrations further resulted in increases in corresponding SOA contributions to annual average total aerosol optical depth (AOD) by <1 % for MZ4-v1 and ~1–6 % for MZ4-v2. Estimated global SOA production was ~6.6 Tg yr^{-1} and ~19.1 Tg yr^{-1} with corresponding burdens of ~0.24 Tg and ~0.59 Tg using MZ4-v1 and MZ4-v2, respectively. The SOA budgets predicted in the current study fall well within reported ranges for similar modeling studies, 6.7 to 96 Tg yr^{-1}, but are lower than recently reported observationally-constrained values, 50 to 380 Tg yr^{-1}. With MZ4-v2, simulated SOA concentrations at the surface were also in reasonable agreement with comparable modeling studies and observations. Concentrations of estimated organic aerosol (OA) at the surface, however, showed under-prediction in Europe and over-prediction in the Amazonian regions and Malaysian Borneo during certain months of the year. Overall, the updated version of MOZART-4, MZ4-v2, showed

GMDD

5, 4187–4232, 2012

consistently better skill in predicting SOA and OA levels and spatial distributions as compared with unmodified MOZART-4. The MZ4-v2 updates may be particularly important when MOZART-4 output is used to generate boundary conditions for regional air quality simulations that require more accurate representation of SOA concentrations and distributions.

1 Introduction

Secondary organic aerosol (SOA) is formed through a series of oxidation reactions of precursor volatile organic compounds (VOCs) followed by partitioning of the oxidation products formed into particles based on their volatilities and activities (see for example, Pankow, 1994; Odum et al., 1996; Kavouras et al., 1998; Claeys et al., 2004; Kanakidou et al., 2005; Hallquist et al., 2009; Jimenez et al., 2009) Organic aerosol (OA), a significant fraction of which is secondary, is a major component of fine particles throughout the atmosphere (Kanakidou et al., 2005). Such particles pose serious health risks (Schwartz, 2004; Delfino et al., 2005; Pope and Dockery, 2006) and affect the global radiative forcing budget (Andreae and Crutzen, 1997; Forster et al., 2007). In an early global SOA modeling study, Chung and Seinfeld (2002) estimated a global annual mean SOA production of 11.2 Tg yr^{-1} considering contributions solely from biogenic VOC precursors (excluding isoprene). Henze and Seinfeld (2006) showed that treating isoprene, which had previously been ignored as an SOA precursor, could double estimated global SOA production (to 16.4 Tg yr^{-1}). More recently, Spracklen et al. (2011) estimated a global annual mean SOA production of 50–380 Tg yr^{-1} from both anthropogenic and biogenic sources, including isoprene. The differences between early global model estimates of SOA production and more current estimates largely are due to changes in the identities and fluxes of the VOC precursors considered, as indicated above, and the SOA processes included, such as partitioning of primary OA and treatment of SOA aging (Lane et al., 2008; Murphy and Pandis, 2009; Farina et al., 2010). For the current generation of global chemical transport models,

GMDD
5, 4187–4232, 2012

model-measurement comparisons show that while OA levels are in good agreement in certain areas (e.g. Heald et al., 2006; Slowik et al., 2010; Lin et al., 2012), models often produce under-estimates, both in the boundary layer (see for example, Johnson et al., 2006; Volkamer et al., 2006; Simpson et al., 2007; Kleinman et al., 2008) and free troposphere (Heald et al., 2011). Heald et al. (2011) showed that though the latest generation of the global chemical transport model GEOS-Chem (Goddard Earth Observing System – Chem) captured general trends in vertical profiles, OA levels were under-estimated in the free troposphere (between ∼ 2–6 km a.g.l.) in 13 out of 17 field campaigns.

The under-prediction of total OA levels by global (and regional) chemical transport models is typically attributed to under-prediction of SOA. The under-prediction of SOA in the atmosphere largely is a consequence of simplified model parameterizations that include a limited number of parent VOCs, as well as an incomplete understanding and representation of the principal mechanisms and products which contribute to SOA formation under ambient conditions. Accurate representations of precursor species and their reactions/reaction products are critical for predicting SOA concentrations in the atmosphere. Thus, there have been numerous efforts to improve SOA parameterizations for regional and global models (Donahue et al., 2006; Pankow and Barsanti, 2009; Lee-Taylor et al., 2011; Murphy et al., 2011; Valorso et al., 2011). Following on previous SOA model improvements, this work seeks to employ updated SOA parameterizations in the global chemical transport model, MOZART-4 (Model for Ozone and Related chemical Tracers, version 4) (Emmons et al., 2010).

MOZART has been employed to estimate global abundance and budgets of air pollutants such as ozone (O_3) (Emmons et al., 2010) and OA (Lack et al., 2004), and to study source attributions (Wespes et al., 2012) and long-range transport of transboundary pollutants (e.g. Park et al., 2009; Pfister et al., 2010; Clarisse et al., 2011). MOZART is also frequently used to generate boundary conditions (BCs) in regional modeling studies (see for example, Dunlea et al., 2009; Tang et al., 2009; Herron-Thorpe et al., 2012). These studies have shown that MOZART-derived dynamic BCs

GMDD
5, 4187–4232, 2012

generally improve predictions, particularly for gas-phase pollutants, as seasonal variations and effects of long-range transport are incorporated. It is expected that with the inclusion of relevant SOA precursors and updated SOA parameters alone, SOA predictions by MOZART can be significantly improved, one important consequence of which will be an improvement in BCs used in regional air quality modeling studies. The current public-release version of MOZART (MOZART-4) calculates SOA based on two-product (2p) parameterizations for a limited number of precursor VOC species. The objective of the current study is to update the SOA module in MOZART-4 by replacing existing 2p parameters with those obtained from 2p volatility basis set (2p-VBS) fits, and by treating additional anthropogenic and biogenic VOCs that are known SOA precursors.

2 Methods

Detailed descriptions of the modeling system and updates to MOZART-4 from previous versions can be found elsewhere (Emmons et al., 2010). Here a brief description of the model and updates to the SOA module are presented.

2.1 Description of the MOZART-4 model

The Model for Ozone and Related chemical Tracers, version 4 (MOZART-4) is an offline global chemical transport model particularly well-suited for studies of the troposphere (Emmons et al., 2010). MOZART-4 has been developed at the National Center for Atmospheric Research (NCAR) and includes a number of updates over the previous version, MOZART-2 (Horowitz et al., 2003). The modeling framework of MOZART is based on an initial model of atmospheric chemistry and transport (MATCH) developed by Rasch et al. (1997). The treatment of physical processes including convective mass flux (Hack, 1994), vertical diffusion within boundary layer (Holtslag and Boville, 1993), wet deposition (Brasseur et al., 1998), and advective transport (Lin and Rood, 1996) in the current version of MOZART have not been updated from MOZART-2. However,

GMDD
5, 4187–4232, 2012

the gas-phase chemical mechanism has been significantly improved in MOZART-4. Tables 2 and 3 in Emmons et al. (2010) explicitly list the model species and gas-phase reactions. There are 85 gas-phase species, 12 bulk aerosol compounds, 39 photolysis and 157 gas-phase reactions in MOZART-4.

The aerosol component of the model includes calculations of sulfate, black carbon, primary organic carbon (i.e. POA) and secondary organic carbon (i.e. SOA), ammonium nitrate and sea salt. The black and organic carbon aerosols are calculated from both hydrophilic and hydrophobic fractions. Sulfate aerosols are calculated from sulfur dioxide and dimethyl sulfide emissions. Uptake of gas-phase dinitrogen pentoxide, hydrogen dioxide radical, nitrogen dioxide and nitrogen trioxide are allowed, and the hygroscopic growth of the aerosol is determined from the ambient relative humidity. The washout of all aerosols is set to 20 % of the washout of nitric acid. The bulk aerosol parameters used in calculation of surface area are provided in Table 6 of Emmons et al. (2010).

MOZART-4 calculates photolysis rates online using the fast-TUV (FTUV) scheme based on the TUV (Tropospheric Ultraviolet-Visible) model that takes into account the impact from clouds and aerosols. The dry deposition of gas- and particle-phase species is also determined online using resistance-based parameterizations of vegetation. Figure 1 shows the steps required to configure, compile and run MOZART-4 on a Linux cluster. Figure 1 also indicates where the model has been updated in this work. A description of the updates to the SOA module is provided below.

2.2 Updates to secondary organic aerosol (SOA) module

The formation of secondary organic aerosol (SOA) in MOZART-4 is linked to gas-phase chemistry through oxidation of various precursor volatile organic compounds (VOCs) including lumped monoterpenes ($C_{10}H_{16}$), lumped aromatics (as toluene), and lumped alkanes with $C > 3$ (BIGALK) through oxidation by hydroxyl radical (OH), O_3 and/or nitrate radical (NO_3). SOA formation is based on the Odum two-product (2p) model (Odum et al., 1996), where products are formed through the gas-phase oxidation

GMDD
5, 4187–4232, 2012

(OXIDANT) reactions of precursor (PARENT) VOCs, and subsequently partition into the particle phase:

$$\text{PARENT} + \text{OXIDANT} \rightarrow \alpha_1 \text{PROD}_1 + \alpha_2 \text{PROD}_2 \quad (1)$$

The fractional yield (α_i) of each lumped VOC oxidation product (e.g. PROD_1 and PROD_2) is obtained from literature. In the current version of the model, the lumped products partition into an existing organic aerosol mass (M_o). The gas/particle partitioning of each lumped product is based on the fundamental theory developed by Pankow (1994). SOA yields (Y_p) are derived instantaneously using Eq. (2) (adapted from Lack et al., 2004) and are dependent on the M_o that exists at that time step:

$$Y_p = M_o \sum_i \left(\frac{\alpha_i K_{p,i}}{1 + K_{p,i} M_o} \right) \quad (2)$$

Partitioning coefficients ($K_{p,i}$) are obtained from literature. The OA can consist of primary and secondary constituents and is obtained from the organic carbon (OC) distributions in the model. If M_o is zero at an initial time step, then the bulk yield method (Lack et al., 2004) is utilized to produce a small amount of M_o that can act as a homogeneous condensation site for SOA.

For the base-case, the existing 2p parameters for each of the default parent VOC species in the model were normalized for particle density of $1\,\text{g}\,\text{cm}^{-3}$ and a standard temperature of 298 K. The SOA module was then updated by replacing the existing 2p parameters with two-product volatility basis set (2p-VBS) parameters, except for isoprene oxidation by OH and lumped monoterpene oxidation by NO_3. The 2p-VBS parameters were conceived in order to take advantage of the robustness of the VBS fitting approach (e.g. see Presto and Donahue, 2006), while allowing the widely-used 2p-modeling framework to be retained. The parameters were derived by: (1) using VBS fits (Tsimpidi et al., 2010) to generate pseudo-data, and (2) fitting the pseudo-data using the 2p approach (Odum et al., 1996). The version of MOZART-4 employing the

GMDD
5, 4187–4232, 2012

2p-VBS parameters henceforth will be called MZ4-v1. Finally, additional SOA precursor species, not previously considered, were treated in the SOA module. The added species were the biogenic precursor isoprene (C_5H_8), and the anthropogenic precursors propene (C_3H_6, "OLE1" in SARPC) and lumped alkenes with $C > 3$ (BIGENE, "OLE2" in SAPRC). This version of MOZART-4 will henceforth be referred to MZ4-v2. Table 1 contains the list of 2p-VBS parameters for the MOZART-4 default precursor species and newly treated species (with the exception of isoprene, for which the parameters of Henze and Seinfeld (2006) were used and monoterpene oxidation by NO_3, for which the parameters of Chung and Seinfeld (2002) were used). Note that the parameters provided in Table 1 are based on high NO_x pathways (anthropogenic precursors) and are for particle density of 1 g cm^{-3} and temperature 298 K to be consistent with the original MOZART-4 parameters.

2.3 Model simulations

In the current study, the MOZART-4 source code was downloaded from the University Cooperation for Atmospheric Research (UCAR) website (http://cdp.ucar.edu). All model simulations were carried out for the entire year of 2006, and the monthly averages were analyzed. Anthropogenic emissions used for the simulation in the current study came from the POET (Precursors of Ozone and their Effects in the Troposphere) dataset for 2000 (Olivier et al., 2003; Granier et al., 2005). Monthly average biomass burning emissions were from the Global Fire Emissions Database, version 2 (GFED-v2) (van der Werf et al., 2006). Biogenic emissions of monoterpenes and isoprene are calculated online in MOZART-4 using the Model of Emissions of Gases and Aerosols from Nature (MEGAN) (Guenther et al., 2006).

MOZART-4 was driven by meteorology from the NCAR reanalysis of the National Centers for Environmental Prediction (NCEP) forecasts (Kalnay et al., 1996; Kistler et al., 2001), at a horizontal resolution of $\sim 2.8^\circ \times 2.8^\circ$, with 28 vertical levels from the surface to ~ 2.7 hPa. This gives a standard resolution of 128×64 grid boxes with

GMDD
5, 4187–4232, 2012

28 vertical layers. The surface and upper boundary conditions for major stable species in the model came from ground-based and satellite measurements.

3 Results and discussion

In this section, analyses from the base-case and updated MOZART-4 simulations are presented followed by comparisons with observations and previous modeling studies. There is no direct measurement of SOA as a component of total OA, thus observational data for global SOA levels are essentially non-existent. Previous studies (see for example, Lack et al., 2004; Heald et al., 2006; Liao et al., 2007; Farina et al., 2010; Jiang et al., 2012; Lin et al., 2012) have compared modeled SOA to SOA determined indirectly from total OA measurements. Some of these studies have also compared modeled SOA with reported SOA levels from relevant modeling studies. It is important to recognize that both of these techniques, comparing modeled levels with indirect determinations and/or with other modeling studies, have limitations. For example, most of the measurements are taken at specific locations over a short period of time. This makes the comparison with global chemical transport model output, predicted monthly averages for a grid cell in the order of degrees, quite difficult and potentially erroneous. Differences in measurement techniques to identify the split between elemental carbon (EC) and organic carbon (OC) in particle samples, required for the indirect determinations of SOA, also contribute to compounding errors in comparisons between modeled vs. calculated SOA. Regarding model to model comparisons, model predictions are also subject to errors which primarily evolve from uncertainties in emissions, meteorology and physical and chemical parameterization techniques unique to each chemical transport model. Nevertheless, such comparisons are necessary for model development and validation.

GMDD
5, 4187–4232, 2012

3.1 Modeled SOA concentrations

3.1.1 Surface concentrations

Figure 2 shows global temporal and spatial distributions of monthly average SOA concentrations ($\mu g\,m^{-3}$) at the surface produced by the base-case simulations. SOA of $> 1.0\,\mu g\,m^{-3}$ is predicted in heavily forested regions in the world including the Amazonian region in South America, equatorial regions in Africa, and rainforest regions in Southeast Asia. The highest amount of SOA, $\sim 3.0\,\mu g\,m^{-3}$, was predicted in the Amazonian region during the month of September, followed by $\sim 2.0\,\mu g\,m^{-3}$ in Indonesia during the month of September and $\sim 2.0\,\mu g\,m^{-3}$ in the equatorial region in Africa in December. The Amazonian region generally experienced ~ 0.6–$2.0\,\mu g\,m^{-3}$ of SOA in other months including March, June and December (the highest monthly concentration, $\sim 9.0\,\mu g\,m^{-3}$ in August, was predicted in the Amazonian region and is not shown in Fig. 2). Similarly, the rainforest regions in Southeast Asia experienced ~ 0.4–$1.0\,\mu g\,m^{-3}$ of SOA during the months of March, June and December. The base-case model predicted ~ 0.2–$0.8\,\mu g\,m^{-3}$ of SOA in the equatorial regions in Africa for months other than December. SOA concentrations of ~ 0.2–$0.6\,\mu g\,m^{-3}$ were predicted in the eastern and western parts of the USA only during the summer months of June and September. Western Europe consistently experienced $\sim 0.2\,\mu g\,m^{-3}$ of SOA formation throughout the year. In Southern and Eastern China, predicted SOA concentrations varied between ~ 0.2 and $\sim 1.4\,\mu g\,m^{-3}$ throughout all seasons. SOA of $\sim 0.2\,\mu g\,m^{-3}$ was predicted over the Indian subcontinent only in December. It is important to note that the global distribution of SOA is primarily dominated by the SOA precursors emitted from biogenic sources, which can be seen from the distributions of precursor VOC emissions as discussed in the following paragraphs.

Figure 3a, b shows global distributions of monthly average surface emissions rates ($mg\,m^{-2}\,day^{-1}$) of summed monoterpenes ($C_{10}H_{16}$) and isoprene (C_5H_8), respectively. The plots reveal that emissions are higher in the Amazonian region in South America, Mid-Africa near the equator, Northeast and Southeast USA, West Europe,

GMDD
5, 4187–4232, 2012

Southeast Asia, South and East China, and Australia compared to other parts of the world. Monoterpene emissions in South America vary between $\sim$ 6–14 mg m^{-2} day^{-1} throughout the year, with highest emissions occurring during the Southern Hemisphere spring (September) and summer (December) months. Consequently, the base-case model also predicted higher amounts of SOA in these regions (Fig. 2) during these months. Emissions in Mid-Africa, Southeast Asia, and Australia vary between $\sim$ 2–8 mg m^{-2} day^{-1} throughout the year. Regions in North America and Europe emit relatively lower amounts of monoterpenes, $<$ 1 µg m^{-2} day^{-1} for spring (March) and winter (December) months, and $\sim$ 1–6 mg m^{-2} day^{-1} for summer (June) and fall (September) months.

Isoprene emissions follow similar spatial and temporal distributions to monoterpenes. Emissions in South American regions vary from $\sim$ 8–56 mg m^{-2} day^{-1}, with the highest levels occurring in their spring month. Isoprene emissions over the Australian continent can be significant, especially in their summer and fall months when the emissions are $\sim$ 10–40 mg m^{-2} day^{-1}. Consistent emissions of isoprene are also found in Southeast Asian regions throughout the year, at rates of $\sim$ 8–28 mg m^{-2} day^{-1}. Generally, isoprene emissions are 4 to 5 times higher than the emissions of monoterpenes; thus even with a relatively low SOA yield (e.g. Lee et al., 2006), the treatment of isoprene as an SOA precursor (as in MZ4-v2) has the potential to substantially change SOA predictions, likely improving global and regional SOA predictions (the latter when MOZART-4 is used to generate boundary conditions).

The amount of SOA produced in the atmosphere largely depends on the concentration of precursors, availability of oxidants, and SOA yields for each of the precursor species; additionally, SOA yields depend on the amount of existing organic aerosol into which compounds can condense. Global surface emissions of primary organic aerosol (POA) and SOA precursors utilized in the current work are given in Table 2. A POA emission rate of 63 Tg yr^{-1} was used for all MOZART-4 simulations, including the base-case. The total SOA precursor emissions were significantly higher in the MZ4-v2 simulation than in the MZ4-v1 and base-case simulations, due to the consideration

GMDD
5, 4187–4232, 2012

of isoprene, BIGENE and C_3H_6. The sum of VOC emissions acting as SOA precursors was 676 Tg yr^{-1} in MZ4-v2, and 199 Tg yr^{-1} in MZ4-v1 and the base-case. Biogenic sources constituted ~ 82 % and ~ 45 %, respectively, of the total SOA precursor emissions; of the 82 % in MZ4-v2, isoprene (ISOP) accounted for ~ 84 % (with summed monoterpenes accounting for the remaining 16 %). Lumped alkanes (BIGALK), with an emission rate of 77 Tg yr^{-1}, were the dominant parent VOC from anthropogenic sources followed by lumped aromatics (TOLUENE: 33 Tg yr^{-1}), lumped alkenes (BIGENE: 9 Tg yr^{-1}) and propene (C_3H_6: 6 Tg yr^{-1}).

The change in SOA (ΔSOA) predicted by the updated versions of MOZART-4, MZ4-v1 and MZ4-v2, was calculated as a fractional change from the base-case as follows: $\Delta SOA_{fractional} = \frac{(SOA_{updated} - SOA_{basecase})}{SOA_{basecase}}$, where $SOA_{updated}$ is the concentration of SOA from the updated version model run, and $SOA_{basecase}$ is the concentration of SOA from the base-case model run. Figure 4 shows the distribution of the fractional change in SOA relative to the base-case as predicted by MZ4-v1. Utilization of the 2p-VBS parameters resulted in significant increases in SOA over the USA in North America, West and Central Europe, and Eastern China in Asia. Monthly average SOA in these regions increased by ~ 1–2 times (~ 100–200 %) throughout the year with slightly higher increases (~ 200–250 %) in the month of December. Generally, the base-case SOA concentrations in these regions was < 1 μg m^{-3}. A consistent SOA increase of ~ 50 % in the months of September and December was seen in the South American and Mid-African regions, where the base-case SOA was in the range of ~ 2–3 μg m^{-3} for those months. Increased SOA in continental North America, Europe, and Asia indicates that anthropogenic precursors such as toluene (TOLUENE) and lumped alkanes (BIGALK) can lead to significant SOA formation, even as represented in a global model, depending on the parameters used.

Figure 5 shows the fractional change in monthly average SOA relative to the base-case as predicted by MZ4-v2. SOA typically increased over some areas in the Eastern USA, West Europe, South and Southeast Asia, and China by as much as ~ 2–4 times (~ 200–400 %); in MZ4-v2, predicted SOA concentrations were ~ 0.1–0.2 μg m^{-3}

GMDD
5, 4187–4232, 2012

throughout the year, except for the month of September which showed higher increases (up to ~ 600 %) in some parts of the USA, China, and South and Southeast Asia. The highest increase of SOA (~ 16–28 times the base-case) was predicted in Northwestern Australia during the months of September and December. In these regions, greater increases in SOA were predicted due to the contribution of isoprene in September and December (which follows the pattern of isoprene emissions at these times of the year in these regions). Given the absence of isoprene as an SOA precursor in the base-case, the corresponding base-case concentrations of SOA in these regions were usually low ~ 0.01–0.04 μg m^{-3}. MZ4-v2 predicted ~ 400–600 % increases in some hotspots in the Amazonian regions in South America throughout the year. Similar increases were also seen in in middle and southern parts of Africa during the months of March, September and December. Again, these patterns of increased SOA followed the patterns of isoprene emissions during corresponding months.

Table 3 contains regionally-averaged annual SOA concentrations at the surface with $\pm 1\sigma$ for several geographic areas around the world for all three versions of model simulations. The area coordinates were adopted from Emmons et al. (2010). The regional averages were calculated based on SOA concentrations in all grid cells over land within the specified coordinates using the global land-mask field. Annual average SOA concentrations varied between 0.06–0.36 μg m^{-3} for the base-case, with the highest concentrations for the specified regions within South America and lowest for the southern regions within Africa. The SOA concentrations were generally high in regions with higher emissions from biogenic sources, in this case, monoterpenes only (e.g. Fig. 2). With MZ4-v1 (SOA parameter updates) the concentration of SOA increased from the base-case between ~ 8–108 %. It is interesting to note that the changes were usually greater for areas where SOA is low, but heavily dominated by anthropogenic emissions. For example, USA, Europe, North Asia and Southeast Asia showed relatively higher SOA increases, ~ 16–108 % (over the base-case). In comparison, SOA increases in regions in South America, Indonesia, Africa, and Australia were generally lower, ~ 8–16 %. (These changes due to parameter updates also are reflected in

GMDD
5, 4187–4232, 2012

Fig. 4.) For the MZ4-v2 simulations (SOA parameter updates and additional SOA precursors) regionally-averaged annual SOA increased from the base-case by as much as ~ 90–600 % (or ~ 0.9–6 times). The increase was attributed mostly to the consideration of isoprene as an SOA precursor, which accounted for ~ 99 % of the total global SOA production in MZ4-v2, compared to the two dominant anthropogenic precursors, namely propene (C_3H_6) and lumped big alkenes (BIGENE). The standard deviation ($\pm 1\sigma$) shows the regional variability in SOA prediction. Higher $\pm 1\sigma$ represents higher variability within the specified regions and vice versa. The source of variability in predicted SOA in this study can be attributed to the variability of regional biogenic emissions (see Fig. 3).

3.1.2 Vertical profiles

Several past and recent studies found that global chemical transport models poorly represent observed concentrations of SOA in the vertical direction (see for example, Heald et al., 2005, 2011; Lin et al., 2012). Efforts were made in the current study to examine how changes in SOA at the surface, driven by updates to the SOA module, translated to the other vertical layers. MOZART-4 has 28-vertical layers extending up to ~ 2.7 hPa (~ 30 km) a.g.l. Figure 6 shows vertical profiles of regionally-averaged annual SOA concentrations for four regions: USA, Indonesia, South America and Japan. The figure shows that updating the SOA parameters (MZ4-v1) had little effect on the vertical profiles compared to the base-case, whereas, treating the additional SOA precursors, namely isoprene, (MZ4-v2), had a significant effect on vertical profiles. The reason for this is likely two-fold, one is just the significant mass production from isoprene, and the other is the relatively high-yield/low-volatility of isoprene SOA product 1, as determined by the fitted α and K_p values shown in Table 1. MZ4-v2 predicted SOA increased by ~ 160 %, ~ 300 %, ~ 170 % and ~ 150 % in the free troposphere (between 801.40–435.70 hPa, ~ 2–6 km) for USA, Indonesia, Japan, and South America from the base-case annual average of 0.03, 0.08, 0.03, and 0.12 $\mu g\, m^{-3}$, respectively.

GMDD
5, 4187–4232, 2012

3.1.3 Global budgets

Estimated global production, deposition, lifetime and atmospheric burden of SOA are presented in Table 5 for all three versions of model simulations. The net production of SOA is assumed to be equal to the net deposition flux, mostly dry and wet deposition, in all simulations. The base-case model estimated SOA production of 5.8 Tg yr^{-1}, while MZ4-v1 and MZ4-v2 estimated 6.6 and 19.1 Tg yr^{-1} of SOA, respectively. Clearly updates to SOA parameters and additional sources enhanced SOA production, which also increased atmospheric burdens by 8 % and 168 %, respectively, from the base-case estimate. Among the three newly treated parent VOC species, isoprene (ISOP) contributed ~ 99 % to additional production of atmospheric SOA through OH oxidation. The current study finds that isoprene, in general, accounts for ~ 65 % of the total SOA formed in the atmosphere. Comparable modeling studies reported that isoprene alone can generate up to 15–75 % of atmospheric SOA (see for example, Heald et al., 2006; Henze and Seinfeld, 2006; Hoyle et al., 2007; Liao et al., 2007; Tsigaridis and Kanakidou, 2007) The base-case model estimated an SOA lifetime of 13.6 days, while the updated versions, MZ4-v1 and MZ4-v2, estimated 13.1 and 11.2 days, respectively. MZ4-v4 calculated an ~ 18 % shorter lifetime likely due to treatment of isoprene as an SOA precursor. Recall that isoprene contributed ~ 99 % to the enhancement of SOA at the surface making contributions from additional anthropogenic precursors less significant in MZ4-v2. The atmospheric lifetimes of biogenic precursors (~ hours) are generally shorter than anthropogenic precursors (~ days) (Farina et al., 2010). Long lifetimes of anthropogenic precursors thus make them more likely to be transported to higher altitudes prior to the formation of SOA, where dry and wet depositions are less efficient (Lin et al., 2012). In MZ4-v2, much of the enhanced SOA are formed within the first few layers (within ~ 500 m a.g.l.) mostly due to inclusion of isoprene in the model (e.g. Fig. 5 vs. Fig. 6), where dry and wet depositions are very effective. This perhaps resulted in shorter lifetime compared to the base-case.

GMDD
5, 4187–4232, 2012

3.2 Model evaluation

The current study found that the use of updated parameters showed little impact on final predicted SOA concentrations and global budget estimates compared to the addition of newly treated parent VOC species (namely isoprene). Hence, only results from the MZ4-v2 simulations are compared here with observations and previous modeling studies. For model-model comparisons, SOA abundance and budget estimates are from models that employed a 2p SOA model approach on a relatively coarse grid (in the order of degrees), unless stated otherwise. For the purpose of measurement-model and model-model comparisons, where necessary, a conversion factor of 1.4 (suggested by Griffin et al., 1999; Russell et al., 2003) was used to convert between organic aerosol mass (OM) and organic carbon mass (OC). Because of the variability in measured and suggested OM : OC values (e.g. from 1.3, Liousse et al., 1996, to 2.2, Zhang et al., 2005) the choice of the OM : OC value is one source of uncertainty in model evaluation. The value of 1.4 used here is on the lower end of the global mean values and thus may bias results toward over-prediction.

3.2.1 Surface SOA

MZ4-v2 predicted increased SOA concentrations at the surface in North America, particularly in the Eastern USA and Europe during the summer months of June, July and August, when the biogenic emissions are at their peak. Using GEOS-Chem, Liao et al. (2007) predicted climatological average (2001–2003) summertime SOA concentrations of ~ 0.5–$2\,\mu g\,m^{-3}$ and ~ 0.5–$1\,\mu g\,m^{-3}$ from isoprene and monoterpene precursors over the Southeastern and Northeastern US, respectively. In the current work, predicted summertime SOA concentrations were ~ 0.9–1.3 and ~ 1.3–$1.4\,\mu g\,m^{-3}$ over the Northeastern and Southeastern US, respectively. Farina et al. (2010) reported that the GISS II GCM predicted SOA reasonably well over Europe. Estimated monthly average OM concentrations were between 8.5 and $8.9\,\mu g\,m^{-3}$ while the observed monthly

GMDD
5, 4187–4232, 2012

average was 6.9 $\mu g\,m^{-3}$ for the period 2002–2003. In the present study, the modeled monthly average OM for the same region (Europe) was $\sim 5.0\,\mu g\,m^{-3}$ for the year 2006.

MZ4-v2 predicted significant increases in SOA in several regions in Asia, including areas within Southeast Asia and eastern parts of China. There are no continuous measurement data available for these regions that can be compared with modeled concentrations. The model comparison is thus limited by the sparse data available for these regions. Robinson et al. (2011) reported a measured OM concentration of 0.74 $\mu g\,m^{-3}$ at the surface in the Malaysian Borneo (4.981° N, 117.844° E) during the Oxidant and Particulate Photochemical Processes above a South East Asian Rainforest (OP3)/Aerosol Coupling in the Earth's System (ACES) project (June–July, 2008). For these two months in summer, MZ4-v2 predicted a monthly average OM of $\sim 2.3\,\mu g\,m^{-3}$ of which ~ 58 % was attributable to SOA mostly derived from isoprene oxidation. This apparent over-prediction may be explained by an erroneously high isoprene SOA yield (for the given ambient conditions) and/or over-estimated emissions rates utilized in the current study. In a recent modeling study, Jiang et al. (2012) estimated annual average SOA concentrations of ~ 2.78 and $\sim 2.92\,\mu g\,m^{-3}$ for areas within South China (22–26° N, 100–115° E) and Central China (25–35° N, 103–120° E), respectively, for the year 2006 using a regional-scale model, WRF-Chem (Weather Research and Forecasting–Chemistry). MZ4-v2 predicted annual average SOA concentrations of 1.11 ± 0.59 and $0.88 \pm 0.42\,\mu g\,m^{-3}$ for South and Central China, respectively. The SOC/OC ratio predicted by MZ4-v2 was ~ 17 % compared to ~ 16 % reported by Jiang et al. (2012) in North China, while observed SOC/OC ratios of ~ 26–59 % have been reported for the Beijing area (Dan et al., 2004; Chan et al., 2005; Duan et al., 2005; Lin et al., 2009). Thus, the updated version of MOZART, MZ4-v2, generally predicted SOA concentrations comparable to other similar modeling studies for regions in China, but over-predicted measured summertime monthly average concentrations in the forested region in Southeast Asia.

Recall that MZ4-v2 predicted generally high SOA concentrations in and around the Amazonian regions in South America. Like regions in Asia, SOA concentration data in

GMDD
5, 4187–4232, 2012

the Amazonian region are also limited and sporadic. Gilardoni et al. (2011) reported a measured OM concentration of 1.70 $\mu g\,m^{-3}$ at the surface in the Amazonian Basin during the wet season (February–June); Chen et al. (2009) reported concentrations of submicron (< 1 µm) OM during February–March period of 0.7 $\mu g\,m^{-3}$. The current study predicted an average OM concentration of ~ 2.15 $\mu g\,m^{-3}$ for the Amazonian region during the wet season. Another modeling study by Lin et al. (2012) predicted an average OM of ~ 3.5 $\mu g\,m^{-3}$ for the same region and season. The modeled concentrations from the current study and Lin et al. (2012) appear to be over-estimating OM in this region. Such over-estimations of OM could be due to an over-estimation of the isoprene SOA yield (for the ambient conditions modeled) and/or an over-estimation of the emissions, of SOA precursors and/or POA, in the region. This discrepancy can also occur due to different meteorology being used in simulations.

3.2.2 Vertical profiles

Several field campaigns have been carried out to understand the abundance of OC, as well as SOA, specifically in the vertical direction. In such campaigns, measurements are typically carried out along flight paths at different altitudes within a specific region of interest. Two of such early major field campaigns were ACE-Asia at the Fukue Island off the coast of Japan in April–May 2001, and ITCT-2K4 over NE North America in July–August of 2004. Data from these campaigns are often utilized to validate model performance in the vertical direction (see for example, Heald et al., 2005, 2006; Lin et al., 2012). Recently, Heald et al. (2011) presented a comprehensive analysis of OA vertical profiles from 17 field campaigns from 2001–2009 (including the two mentioned above) in order to validate model performance on a global scale. In this study, comparisons of modeled vertical profiles were limited to the early field campaigns over the Northwest Pacific (ACE-Asia) and the Northeast of North America (ITCT-2K4).

Heald et al. (2005) reported that GEOS-Chem under-predicted OC, of which SOA is a dominant component, by as much as 10–100 times during the ACE-Asia (2001) study near the coast of Japan (23–43° N, 120–145° E). MZ4-v2 in the current study

GMDD
5, 4187–4232, 2012

predicted a seasonal (April–May) OC aerosol mass of $0.58 \pm 0.24\,\mu g\,C\,m^{-3}$ in the free troposphere (FT) averaged over all the grid cells within the area boundary at model resolution, of which ~16% was attributed to SOA; the observed seasonal average OC mass along the fight paths was $3.3 \pm 2.8\,\mu g\,C\,m^{-3}$. The predicted OC mass concentration in the current study showed a significant improvement from the reported maximum modeled value of $0.30 \pm 0.3\,\mu g\,C\,m^{-3}$ by Heald et al. (2005) averaged over the grid cells along the flight paths. It is worth noting that the Heald et al. (2005) treated monoterpenes as the only biogenic VOC precursor, whereas MZ4-v2 includes both monoterpenes and isoprene. The model prediction in the current study is comparable with the FT average modeled OC aerosol mass of $\sim 0.7\,\mu g\,C\,m^{-3}$ (STP) reported by Lin et al. (2012) for the ACE-Asia field campaign; similarly to this work, Lin et al. (2012) considered isoprene and monoterpenes as major biogenic precursors.

During the ITCT-2K4 campaign (25–55° N, 270–310° E) over summer months July–August, aircraft measurements included those within a large plume that originated from boreal forest fires in Alaska and Canada. Chemical transport models often miss such plumes resulting in significant under-prediction of OM. Heald et al. (2006) reported observed water soluble organic carbon (WSOC) concentrations of $0.9 \pm 0.9\,\mu g\,C\,m^{-3}$ in the FT averaged along the flight paths outside of the boreal forest fire plume, and a corresponding modeled WSOC concentration of $0.7 \pm 0.6\,\mu g\,C\,m^{-3}$ averaged from only grid cells along the flight paths at model resolution. In the current study, MZ4-v2 predicted seasonal WSOC aerosol mass of $0.36 \pm 0.15\,\mu g\,C\,m^{-3}$, of which 21 % was attributable to SOA, in the FT averaged from all grid cells within the region boundary specified. The apparent difference in model prediction between the current study and Heald et al. (2006) might have been due to differences in how the average results are calculated, although both studies included monoterpenes and isoprene as major biogenic precursors with similar emission strengths.

GMDD
5, 4187–4232, 2012

3.2.3 Global budgets

There is significant uncertainty in global SOA budget estimates. A wide range of SOA production rates, measurement and model based, can be found in the literature. For example, Goldstein and Galbally (2007) estimated SOA production of 510–910 $\mathrm{Tg\,C\,yr^{-1}}$ based on a top-down VOC mass balance approach. Global model estimates of SOA production typically span a lower range, from 6.74 $\mathrm{Tg\,yr^{-1}}$ (Goto et al., 2008) to 96 $\mathrm{Tg\,yr^{-1}}$ (Guillaume et al., 2007). The differences in SOA production and atmospheric burden among these model estimates predominantly come from differences in source emissions, choice of SOA parameters, and treatment of parent VOCs in SOA models. Thus SOA production, lifetime and corresponding atmospheric burden estimates from the current study can only rationally be compared with estimates from global chemical transport models that at a minimum utilize a 2p SOA model approach, treat both biogenic (isoprene and monoterpenes) and anthropogenic (mostly aromatics) precursors, generate biogenic emissions using MEGAN, and employ chemical and physical processes similar to the current study. Even controlling for these model differences, it is important to recognize that there are further explicit and/or implicit differences between models that can lead to significant discrepancies in model predictions, further complicating model-model comparisons required for model development and testing.

The updated model, MZ4-v2, estimated global SOA production of 19.1 $\mathrm{Tg\,yr^{-1}}$ with a lifetime of 11.2 days and corresponding atmospheric burden of 0.59 Tg, which falls well within the reported range of model estimates cited above. Recently O'Donnell et al. (2011) estimated global SOA production of 26.6 $\mathrm{Tg\,yr^{-1}}$ with a lifetime of 11.4 days and corresponding global burden of 0.83 Tg, which are in close agreement with the estimates in this work. O'Donnell et al. (2011) utilized the ECHAM5-HAM global model, which, like MOZART-4, also assumes the net deposition of SOA equals the net production of SOA in the atmosphere, although the ECHAM5 model includes sedimentation of SOA as an additional sink process. Differences in dry and wet

GMDD
5, 4187–4232, 2012

deposition schemes and the additional sink process through sedimentation might have resulted in higher production of SOA in O'Donnell et al. (2011) compared to the current study. An earlier study by Henze et al. (2008) estimated global SOA production of 30.3 Tg yr^{-1} using the GEOS-Chem model. The higher global SOA production in Henze et al. (2008) can be attributed to the inclusion of NO_x dependent SOA formation pathways for anthropogenic precursors (not currently an option in the MOZART-4 SOA module) and treatment of additional SOA precursors (benzene, alcohols and sesquiterpenes). All of these model estimates are significantly lower than the observationally-constrained top-down estimates (50–380 Tg yr^{-1}) of Spracklen et al. (2011).

3.3 Aerosol optical depth (AOD)

Figure 7 shows a measure of the total aerosol optical depth (AOD) for the base-case MOZART-4 simulations. The monthly-averaged total AOD presented here includes contributions from primary and secondary organic carbon (OC), black carbon (BC), dust, sea-salt, and sulfate and nitrate particles. As shown in Fig. 7, AOD is generally higher for the Northern Hemisphere than the Southern Hemisphere, supporting that primary anthropogenic particulate emissions (e.g. BC) and dust are the largest contributors to modeled AOD; this is in contrast to the significant contribution of biogenic emissions to total particulate loadings through SOA formation. High AOD ($>\sim 2.0$) over Northern Africa reflects large contributions ($\sim 80\,\%$) from dust particles, and over Southeastern China from anthropogenic sources ($>\sim 90\,\%$) including BC, sulfate, nitrate and OC. However, the contribution of OC to total AOD is generally $<\sim 20\,\%$ in the modeled regions (Table 4).

Figure 8 shows the relative increase ($\Delta AOD_{fractional} = \frac{(AOD_{updated} - AOD_{basecase})}{AOD_{basecase}}$) in total AOD due to the updates in MZ4-v2. The increase in AOD is in the range of ~ 1–$7\,\%$ in areas where SOA production also increased due to treatment of additional SOA precursor VOCs (e.g. Fig. 5). To illustrate further that anthropogenic aerosols dominate AOD, regionally-averaged annual AOD was calculated for several regions including

GMDD
5, 4187–4232, 2012

major oceans of the world. Table 4 shows regionally-averaged base-case annual total AOD, contributions from POA and SOA, and change in total AOD attributed to additional SOA formed in the MZ4-v2 simulations. The table contains total AOD analysis for the regions for which SOA was also averaged annually (Table 3). Additionally, annual total AOD results over oceans are presented. Note that the AOD over oceans was calculated using oceans only grid cells within the boundary coordinates. Generally, AOD was much higher over land compared to over oceans because sources are located over land. The base-case model predicted the highest annual average total AOD of 0.73 over North Africa, of which ~ 80 % is attributed to dust; only 3 % is attributed to POA and SOA. MZ4-v2 predicted POA and SOA contributed ~ 3–21 % to total AOD over the regions considered in the current study. Regionally-averaged annual total AOD increased by ~ 0.6–8.2 % due to additional SOA formed in the MZ4-v2 simulation. The model predicted that AOD increased over areas where SOA also increased from the base-case prediction. For example, Australia, Indonesia and South America experienced ~ 750 %, ~ 400 % and ~ 300 % increases in SOA which contributed to increases in total AOD by ~ 7.7 %, 4.4 %, and 6.2 %, respectively. Increased SOA resulted in ~ 2.3–8.2 % increase in AOD over the Atlantic, Pacific and Indian Oceans. The South Pacific Ocean experienced the highest AOD increase of 8.2 % predicted by MZ4-v2.

There has been little effort to evaluate AOD predicted by MOZART-4, with the exception of the Emmons et al. (2010) study. In that study, MODIS retrievals were used to evaluate predicted monthly average total AOD over major oceans for several years of retrievals/model simulations. Comparisons for 2006 showed that the modeled AOD fell within the variability bounds of retrieved total AOD for each region of interest. Predicted monthly average total AOD (the base-case MOZART-4 AOD in this work) agreed quite well with observations over the North Pacific Ocean, under-estimated AOD over the South Pacific, South Atlantic, and Indian Oceans, and over-estimated AOD over the North Atlantic Ocean. In the current study, MZ4-v2 predicted ~ 2–8 % increases in the annual total AOD over these oceans, suggesting that the model updates bring the

GMDD
5, 4187–4232, 2012

under-estimated monthly average AOD closer to observations, except over the North Atlantic Ocean where the base-case model already over-estimated AOD.

4 Conclusions

The secondary organic aerosol (SOA) module in the MOZART-4 global chemical transport model was updated by replacing the existing two-product (2p) parameters with those obtained from recent two-product volatility basis set (2p-VBS) fits, and by adding isoprene (C_5H_8), propene (C_3H_6) and lumped alkenes with C > 3 (BIGENE) as precursor VOCs contributing to SOA formation. The base-case simulation predicted annual average SOA of $0.36 \pm 0.50\,\mu g\,m^{-3}$ in South America, $0.31 \pm 0.38\,\mu g\,m^{-3}$ in Indonesia, $0.09 \pm 05\,\mu g\,m^{-3}$ in the USA, and $0.12 \pm 0.07\,\mu g\,m^{-3}$ in Europe. The updates in the 2p parameters alone (MZ4-v1) increased annual average SOA by ~ 8 %, ~ 16 %, ~ 56 %, and ~ 108 % from the base-case in South America, Indonesia, USA, and Europe, respectively. Treatment of additional parent VOCs with 2p-VBS parameters in the model (MZ4-v2) shows even more dramatic increase in annual average SOA for these regions. SOA increases by ~ 178 %, ~ 406 %, ~ 311 %, and ~ 292 % from the base-case predicted concentration in South America, Indonesia, USA and Europe, respectively. The elevated SOA concentrations predicted by MZ4-v2 in these regions further resulted in increases in corresponding SOA contributions to annual average total AOD by ~ 1–6 %. The current study estimated global production of ~ 6.6–19.1 Tg yr^{-1} SOA with corresponding burdens of ~ 0.24–0.59 Tg and lifetimes of ~ 13.1–13.6 days by the updated versions of MOZART-4, which fall within published estimates in previous work by others. Monthly, seasonal and annual averages of SOA and OA concentrations from MZ4-v2 were compared with observations and other similar global chemical transport model predictions. The analysis showed that the concentrations of SOA and OA at the boundary layer in the current study are quite comparable to published model studies that utilized a two-product (2p) SOA model and included at least monoterpenes and isoprene as SOA precursors. MZ4-v2 potentially over-predicted organic mass in

GMDD
5, 4187–4232, 2012

major tropical forests, including the Amazonian basin and Malaysian Borneo, where the model predicted $\sim 2.15\,\mu g\,m^{-3}$ vs. measured $1.70\,\mu g\,m^{-3}$, and $\sim 2.3\,\mu g\,m^{-3}$ vs. measured $0.74\,\mu g\,m^{-3}$, respectively. The SOA contributions to the predicted total organic aerosol mass were ~ 34–58 % over these tropical forests, which imply that the over-prediction might have resulted from high SOA yield for isoprene and/or from overestimation of emissions rates in the inventories utilized in the current study. The modeled concentrations, however, were slightly lower than the estimates from other modeling studies over the same regions. MZ4-v2 slightly under-predicted organic aerosol mass for USA, Europe, and China. MZ4-v2 also under-predicted organic mass in the free troposphere (~ 2–6 km), but clearly showed improvements from previous work bringing modeled estimates closer to observations.

In this work, updates to SOA parameters and treatment of additional precursors not considered in the original SOA module, improved model MOZART-4 predictions of SOA at the surface and in the vertical direction. The modifications to the SOA module in MOZART-4 are scientifically relevant and important for future studies utilizing MOZART-4, including those directed at global SOA and OA budget estimations and pollution source attribution. The modifications to the SOA module also will produce improvements in regional air quality models where MOZART output is used for boundary conditions.

Acknowledgements. This work was supported by the Cooley Family Fund for Critical Research of the Oregon Community Foundation and Research and Sponsored Projects, and the Institute of Sustainable Solutions at Portland State University.

References

Andreae, M. O. and Crutzen, P. J.: Atmospheric aerosols: biogeochemical sources and role in atmospheric chemistry, Science, 276, 5315, doi:10.1126/science.276.5315.1052, 1997.

Brasseur, G. P., Hauglustaine, D. A., Walters, S., Rasch, P. J., Muller, J. F., Granier, C., and Tie, X. X.: MOZART, a global chemical transport model for ozone and related chemical

GMDD

5, 4187–4232, 2012

tracers 1. Model description, J. Geophys. Res., 103, 28265–28289, doi:10.1029/98jd02397, 1998.
Chan, C. Y., Xu, X. D., Li, Y. S., Wong, K. H., Ding, G. A., Chan, L. Y., and Cheng, X. H.: Characteristics of vertical profiles and sources of $PM_{2.5}$, PM_{10} and carbonaceous species in Beijing, Atmos. Environ., 39, 5113–5124, doi:10.1016/j.atmosenv.2005.05.009, 2005.
Chen, Q., Farmer, D. K., Schneider, J., Zorn, S. R., Heald, C. L., Karl, T. G., Guenther, A., Allan, J. D., Robinson, N., Coe, H., Kimmel, J. R., Pauliquevis, T., Borrmann, S., Poeschl, U., Andreae, M. O., Artaxo, P., Jimenez, J. L., and Martin, S. T.: Mass spectral characterization of submicron biogenic organic particles in the Amazon Basin, Geophys. Res. Lett., 36, L20806, doi:10.1029/2009gl039880, 2009.
Chung, S. H. and Seinfeld, J. H.: Global distribution and climate forcing of carbonaceous aerosols, J. Geophys. Res., 107, 4407, doi:10.1029/2001jd001397, 2002.
Claeys, M., Wang, W., Ion, A. C., Kourtchev, I., Gelencser, A., and Maenhaut, W.: Formation of secondary organic aerosols from isoprene and its gas-phase oxidation products through reaction with hydrogen peroxide, Atmos. Environ., 38, 4093–4098, doi:10.1016/j.atmosenv.2004.06.001, 2004.
Clarisse, L., Fromm, M., Ngadi, Y., Emmons, L., Clerbaux, C., Hurtmans, D., and Coheur, P.-F.: Intercontinental transport of anthropogenic sulfur dioxide and other pollutants: an infrared remote sensing case study, Geophys. Res. Lett., 38, L19806, doi:10.1029/2011gl048976, 2011.
Dan, M., Zhuang, G. S., Li, X. X., Tao, H. R., and Zhuang, Y. H.: The characteristics of carbonaceous species and their sources in $PM_{2.5}$ in Beijing, Atmos. Environ., 38, 3443–3452, doi:10.1016/j.atmosenv.2004.02.052, 2004.
Delfino, R. J., Sioutas, C., and Malik, S.: Potential role of ultrafine particles in associations between airborne particle mass and cardiovascular health, Environ. Health Persp., 113, 934–946, doi:10.1289/ehp.7938, 2005.
Donahue, N. M., Robinson, A. L., Stanier, C. O., and Pandis, S. N.: Coupled partitioning, dilution, and chemical aging of semivolatile organics, Environ. Sci. Technol., 40, 2635–2643, doi:10.1021/es052297c, 2006.
Duan, F. K., He, K. B., Ma, Y. L., Jia, Y. T., Yang, F. M., Lei, Y., Tanaka, S., and Okuta, T.: Characteristics of carbonaceous aerosols in Beijing, China, Chemosphere, 60, 355–364, doi:10.1016/j.chemosphere.2004.12.035, 2005.

GMDD
5, 4187–4232, 2012

Dunlea, E. J., DeCarlo, P. F., Aiken, A. C., Kimmel, J. R., Peltier, R. E., Weber, R. J., Tomlinson, J., Collins, D. R., Shinozuka, Y., McNaughton, C. S., Howell, S. G., Clarke, A. D., Emmons, L. K., Apel, E. C., Pfister, G. G., van Donkelaar, A., Martin, R. V., Millet, D. B., Heald, C. L., and Jimenez, J. L.: Evolution of Asian aerosols during transpacific transport in INTEX-B, Atmos. Chem. Phys., 9, 7257–7287, doi:10.5194/acp-9-7257-2009, 2009.

Emmons, L. K., Walters, S., Hess, P. G., Lamarque, J.-F., Pfister, G. G., Fillmore, D., Granier, C., Guenther, A., Kinnison, D., Laepple, T., Orlando, J., Tie, X., Tyndall, G., Wiedinmyer, C., Baughcum, S. L., and Kloster, S.: Description and evaluation of the Model for Ozone and Related chemical Tracers, version 4 (MOZART-4), Geosci. Model Dev., 3, 43–67, doi:10.5194/gmd-3-43-2010, 2010.

Farina, S. C., Adams, P. J., and Pandis, S. N.: Modeling global secondary organic aerosol formation and processing with the volatility basis set: implications for anthropogenic secondary organic aerosol, J. Geophys. Res., 115, D09202, doi:10.1029/2009jd013046, 2010.

Forster, P., Ramaswamy, V., Artaxo, P., Berntsen, T., Betts, R., Fahey, D. W., Haywood, J., Lean, J., Lowe, D. C., Myhre, G., Nganga, J., Prinn, R., Raga, G., Schulz, M., and Van Dorland, R.: Changes in Atmospheric Constituents and in Radiative Forcing, in: Climate Change 2007: the Physical Science Basis. Contribution of Working Group I to the Fourth Assessment Report of the Intergovernmental Panel on Climate Change, edited by: Solomon, S., Qin, D., Manning, M., Chen, Z., Marquis, M., Averyt, K. B.,Tignor, M., and Miller, H. L., Cambridge University Press, Cambridge, UK and New York, NY, USA, 2007.

Gilardoni, S., Vignati, E., Marmer, E., Cavalli, F., Belis, C., Gianelle, V., Loureiro, A., and Artaxo, P.: Sources of carbonaceous aerosol in the Amazon basin, Atmos. Chem. Phys., 11, 2747–2764, doi:10.5194/acp-11-2747-2011, 2011.

Goldstein, A. H. and Galbally, I. E.: Known and unexplored organic constituents in the earth's atmosphere, Environ. Sci. Technol., 41, 1514–1521, doi:10.1021/es072476p, 2007.

Goto, D., Takemura, T., and Nakajima, T.: Importance of global aerosol modeling including secondary organic aerosol formed from monoterpene, J. Geophys. Res., 113, D07205, doi:10.1029/2007jd009019, 2008.

Granier, C., Guenther, A., Lamarque, J., Mieville, A., Muller, J., Olivier, J., Orlando, J., Peters, J., Petron, G., Tyndall, G., and Wallens, S.: POET, a database of surface emissions of ozone precursors, available at: http://www.aero.jussieu.fr/projet/ACCENT/POET.php (last access: August 2008), 2005.

GMDD
5, 4187–4232, 2012

Griffin, R. J., Cocker, D. R., Flagan, R. C., and Seinfeld, J. H.: Organic aerosol formation from the oxidation of biogenic hydrocarbons, J. Geophys. Res., 104, 3555–3567, doi:10.1029/1998jd100049, 1999.

Guenther, A., Karl, T., Harley, P., Wiedinmyer, C., Palmer, P. I., and Geron, C.: Estimates of global terrestrial isoprene emissions using MEGAN (Model of Emissions of Gases and Aerosols from Nature), Atmos. Chem. Phys., 6, 3181–3210, doi:10.5194/acp-6-3181-2006, 2006.

Guillaume, B., Liousse, C., Rosset, R., Cachier, H., Van Velthoven, P., Bessagnet, B., and Poisson, N.: ORISAM-TM4: a new global sectional multi-component aerosol model including SOA formation – focus on carbonaceous BC and OC aerosols, Tellus B, 59, 283–302, doi:10.1111/j.1600-0889.2006.00246.x, 2007.

Hack, J. J.: Parameterization of moist convection in the National Center for Atmospheric Research community climate model (CCM2), J. Geophys. Res., 99, D3, doi:10.1029/93jd03478, 1994.

Hallquist, M., Wenger, J. C., Baltensperger, U., Rudich, Y., Simpson, D., Claeys, M., Dommen, J., Donahue, N. M., George, C., Goldstein, A. H., Hamilton, J. F., Herrmann, H., Hoffmann, T., Iinuma, Y., Jang, M., Jenkin, M. E., Jimenez, J. L., Kiendler-Scharr, A., Maenhaut, W., McFiggans, G., Mentel, Th. F., Monod, A., Prévôt, A. S. H., Seinfeld, J. H., Surratt, J. D., Szmigielski, R., and Wildt, J.: The formation, properties and impact of secondary organic aerosol: current and emerging issues, Atmos. Chem. Phys., 9, 5155–5236, doi:10.5194/acp-9-5155-2009, 2009.

Heald, C. L., Jacob, D. J., Park, R. J., Russell, L. M., Huebert, B. J., Seinfeld, J. H., Liao, H., and Weber, R. J.: A large organic aerosol source in the free troposphere missing from current models, Geophys. Res. Lett., 32, L18809, doi:10.1029/2005gl023831, 2005.

Heald, C. L., Jacob, D. J., Turquety, S., Hudman, R. C., Weber, R. J., Sullivan, A. P., Peltier, R. E., Atlas, E. L., de Gouw, J. A., Warneke, C., Holloway, J. S., Neuman, J. A., Flocke, F. M., and Seinfeld, J. H.: Concentrations and sources of organic carbon aerosols in the free troposphere over North America, J. Geophys. Res., 111, D23S47, doi:10.1029/2006jd007705, 2006.

Heald, C. L., Coe, H., Jimenez, J. L., Weber, R. J., Bahreini, R., Middlebrook, A. M., Russell, L. M., Jolleys, M., Fu, T.-M., Allan, J. D., Bower, K. N., Capes, G., Crosier, J., Morgan, W. T., Robinson, N. H., Williams, P. I., Cubison, M. J., DeCarlo, P. F., and Dunlea, E. J.: Exploring the vertical profile of atmospheric organic aerosol: comparing 17 aircraft field cam-

GMDD

5, 4187–4232, 2012

paigns with a global model, Atmos. Chem. Phys., 11, 12673–12696, doi:10.5194/acp-11-12673-2011, 2011.
Henze, D. K. and Seinfeld, J. H.: Global secondary organic aerosol from isoprene oxidation, Geophys. Res. Lett., 33, L09812, doi:10.1029/2006gl025976, 2006.
Henze, D. K., Seinfeld, J. H., Ng, N. L., Kroll, J. H., Fu, T.-M., Jacob, D. J., and Heald, C. L.: Global modeling of secondary organic aerosol formation from aromatic hydrocarbons: high-vs. low-yield pathways, Atmos. Chem. Phys., 8, 2405–2420, doi:10.5194/acp-8-2405-2008, 2008.
Herron-Thorpe, F. L., Mount, G. H., Emmons, L. K., Lamb, B. K., Chung, S. H., and Vaughan, J. K.: Regional air-quality forecasting for the Pacific Northwest using MOPITT/TERRA assimilated carbon monoxide MOZART-4 forecasts as a near real-time boundary condition, Atmos. Chem. Phys., 12, 5603–5615, doi:10.5194/acp-12-5603-2012, 2012.
Holtslag, A. A. M. and Boville, B. A.: Local versus nonlocal boundary-layer diffusion in a global climate model, J. Climate, 6, 1825–1842, 1993.
Horowitz, L. W., Walters, S., Mauzerall, D. L., Emmons, L. K., Rasch, P. J., Granier, C., Tie, X. X., Lamarque, J. F., Schultz, M. G., Tyndall, G. S., Orlando, J. J., and Brasseur, G. P.: A global simulation of tropospheric ozone and related tracers: description and evaluation of MOZART, version 2, J. Geophys. Res., 108, 4784, doi:10.1029/2002jd002853, 2003.
Hoyle, C. R., Berntsen, T., Myhre, G., and Isaksen, I. S. A.: Secondary organic aerosol in the global aerosol – chemical transport model Oslo CTM2, Atmos. Chem. Phys., 7, 5675–5694, doi:10.5194/acp-7-5675-2007, 2007.
Jiang, F., Liu, Q., Huang, X., Wang, T., Zhuang, B., and Xie, M.: Regional modeling of secondary organic aerosol over China using WRF/Chem, J.Aerosol Sci., 43, 57–73, doi:10.1016/j.jaerosci.2011.09.003, 2012.
Jimenez, J. L., Canagaratna, M. R., Donahue, N. M., Prevot, A. S. H., Zhang, Q., Kroll, J. H., DeCarlo, P. F., Allan, J. D., Coe, H., Ng, N. L., Aiken, A. C., Docherty, K. S., Ulbrich, I. M., Grieshop, A. P., Robinson, A. L., Duplissy, J., Smith, J. D., Wilson, K. R., Lanz, V. A., Hueglin, C., Sun, Y. L., Tian, J., Laaksonen, A., Raatikainen, T., Rautiainen, J., Vaattovaara, P., Ehn, M., Kulmala, M., Tomlinson, J. M., Collins, D. R., Cubison, M. J., Dunlea, E. J., Huffman, J. A., Onasch, T. B., Alfarra, M. R., Williams, P. I., Bower, K., Kondo, Y., Schneider, J., Drewnick, F., Borrmann, S., Weimer, S., Demerjian, K., Salcedo, D., Cottrell, L., Griffin, R., Takami, A., Miyoshi, T., Hatakeyama, S., Shimono, A., Sun, J. Y., Zhang, Y. M., Dzepina, K., Kimmel, J. R., Sueper, D., Jayne, J. T., Herndon, S. C., Trim-

GMDD
5, 4187–4232, 2012

born, A. M., Williams, L. R., Wood, E. C., Middlebrook, A. M., Kolb, C. E., Baltensperger, U., and Worsnop, D. R.: Evolution of Organic Aerosols in the Atmosphere, Science, 326, 5959, doi:10.1126/science.1180353, 2009.

Johnson, D., Utembe, S. R., Jenkin, M. E., Derwent, R. G., Hayman, G. D., Alfarra, M. R., Coe, H., and McFiggans, G.: Simulating regional scale secondary organic aerosol formation during the TORCH 2003 campaign in the southern UK, Atmos. Chem. Phys., 6, 403–418, doi:10.5194/acp-6-403-2006, 2006.

Kalnay, E., Kanamitsu, M., Kistler, R., Collins, W., Deaven, D., Gandin, L., Iredell, M., Saha, S., White, G., Woollen, J., Zhu, Y., Chelliah, M., Ebisuzaki, W., Higgins, W., Janowiak, J., Mo, K. C., Ropelewski, C., Wang, J., Leetmaa, A., Reynolds, R., Jenne, R., and Joseph, D.: The NCEP/NCAR 40-yr reanalysis project, B. Am. Meteorol. Soc., 77, 437–471, doi:10.1175/1520-0477(1996)077<0437:tnyrp>2.0.co;2, 1996.

Kanakidou, M., Seinfeld, J. H., Pandis, S. N., Barnes, I., Dentener, F. J., Facchini, M. C., Van Dingenen, R., Ervens, B., Nenes, A., Nielsen, C. J., Swietlicki, E., Putaud, J. P., Balkanski, Y., Fuzzi, S., Horth, J., Moortgat, G. K., Winterhalter, R., Myhre, C. E. L., Tsigaridis, K., Vignati, E., Stephanou, E. G., and Wilson, J.: Organic aerosol and global climate modelling: a review, Atmos. Chem. Phys., 5, 1053–1123, doi:10.5194/acp-5-1053-2005, 2005.

Kavouras, I. G., Mihalopoulos, N., and Stephanou, E. G.: Formation of atmospheric particles from organic acids produced by forests, Nature, 395, 683–686, doi:10.1038/27179, 1998.

Kistler, R., Kalnay, E., Collins, W., Saha, S., White, G., Woollen, J., Chelliah, M., Ebisuzaki, W., Kanamitsu, M., Kousky, V., van den Dool, H., Jenne, R., and Fiorino, M.: The NCEP-NCAR 50-yr reanalysis: monthly means CD-ROM and documentation, B. Am. Meteorol. Soc., 82, 247–267, doi:10.1175/1520-0477(2001)082<0247:tnnyrm>2.3.co;2, 2001.

Kleinman, L. I., Springston, S. R., Daum, P. H., Lee, Y.-N., Nunnermacker, L. J., Senum, G. I., Wang, J., Weinstein-Lloyd, J., Alexander, M. L., Hubbe, J., Ortega, J., Canagaratna, M. R., and Jayne, J.: The time evolution of aerosol composition over the Mexico City plateau, Atmos. Chem. Phys., 8, 1559–1575, doi:10.5194/acp-8-1559-2008, 2008.

Lack, D. A., Tie, X. X., Bofinger, N. D., Wiegand, A. N., and Madronich, S.: Seasonal variability of secondary organic aerosol: a global modeling study, J. Geophys. Res., 109, D03203, doi:10.1029/2003jd003418, 2004.

Lane, T. E., Donahue, N. M., and Pandis, S. N.: Simulating secondary organic aerosol formation using the volatility basis-set approach in a chemical transport model, Atmos. Environ., 42, 7439–7451, doi:10.1016/j.atmosenv.2008.06.026, 2008.

GMDD
5, 4187–4232, 2012

Lee, A., Goldstein, A. H., Kroll, J. H., Ng, N. L., Varutbangkul, V., Flagan, R. C., and Seinfeld, J. H.: Gas-phase products and secondary aerosol yields from the photooxidation of 16 different terpenes, J. Geophys. Res., 111, D17305, doi:10.1029/2006jd007050, 2006.

Lee-Taylor, J., Madronich, S., Aumont, B., Baker, A., Camredon, M., Hodzic, A., Tyndall, G. S., Apel, E., and Zaveri, R. A.: Explicit modeling of organic chemistry and secondary organic aerosol partitioning for Mexico City and its outflow plume, Atmos. Chem. Phys., 11, 13219–13241, doi:10.5194/acp-11-13219-2011, 2011.

Liao, H., Henze, D. K., Seinfeld, J. H., Wu, S., and Mickley, L. J.: Biogenic secondary organic aerosol over the United States: comparison of climatological simulations with observations, J. Geophys. Res., 112, D06201, doi:10.1029/2006jd007813, 2007.

Lin, G., Penner, J. E., Sillman, S., Taraborrelli, D., and Lelieveld, J.: Global modeling of SOA formation from dicarbonyls, epoxides, organic nitrates and peroxides, Atmos. Chem. Phys., 12, 4743–4774, doi:10.5194/acp-12-4743-2012, 2012.

Lin, P., Hu, M., Deng, Z., Slanina, J., Han, S., Kondo, Y., Takegawa, N., Miyazaki, Y., Zhao, Y., and Sugimoto, N.: Seasonal and diurnal variations of organic carbon in $PM_{2.5}$ in Beijing and the estimation of secondary organic carbon, J. Geophys. Res., 114, D00G11, doi:10.1029/2008jd010902, 2009.

Lin, S. J., and Rood, R. B.: Multidimensional flux-form semi-Lagrangian transport schemes, Mon. Weather Rev., 124, 2046–2070, doi:10.1175/1520-0493(1996)124<2046:mffslt>2.0.co;2, 1996.

Liousse, C., Penner, J. E., Chuang, C., Walton, J. J., Eddleman, H., and Cachier, H.: A global three-dimensional model study of carbonaceous aerosols, J. Geophys. Res., 101, D14, doi:10.1029/95jd03426, 1996.

Murphy, B. N., and Pandis, S. N.: Simulating the formation of semivolatile primary and secondary organic aerosol in a regional chemical transport model, Environ. Sci. Technol., 43, 4722–4728, doi:10.1021/es803168a, 2009.

Murphy, B. N., Donahue, N. M., Fountoukis, C., and Pandis, S. N.: Simulating the oxygen content of ambient organic aerosol with the 2D volatility basis set, Atmos. Chem. Phys., 11, 7859–7873, doi:10.5194/acp-11-7859-2011, 2011.

O'Donnell, D., Tsigaridis, K., and Feichter, J.: Estimating the direct and indirect effects of secondary organic aerosols using ECHAM5-HAM, Atmos. Chem. Phys., 11, 8635–8659, doi:10.5194/acp-11-8635-2011, 2011.

GMDD
5, 4187–4232, 2012

Odum, J. R., Hoffmann, T., Bowman, F., Collins, D., Flagan, R. C., and Seinfeld, J. H.: Gas/particle partitioning and secondary organic aerosol yields, Environ. Sci. Technol., 30, 2580–2585, doi:10.1021/es950943+, 1996.

Olivier, J., Peters, J., Granier, C., Petron, G., Müller, J., and Wallens, S.: Present and future surface emissions of atmospheric compounds, POET report #2, EU project EVK2–1999-00011, available at: http://www.aero.jussieu.fr/projet/ACCENT/POE~T.php (last access: August 2008), 2003.

Pankow, J. F.: An absorption-model of the gas aerosol partitioning involved in the formation of secondary organic aerosol, Atmos. Environ., 28, 185–188, doi:10.1016/1352-2310(94)90094-9, 1994.

Pankow, J. F., and Barsanti, K. C.: The carbon number-polarity grid: a means to manage the complexity of the mix of organic compounds when modeling atmospheric organic particulate matter, Atmos. Environ., 43, 2829–2835, doi:10.1016/j.atmosenv.2008.12.050, 2009.

Park, M., Randel, W. J., Emmons, L. K., and Livesey, N. J.: Transport pathways of carbon monoxide in the Asian summer monsoon diagnosed from Model of Ozone and Related Tracers (MOZART), J. Geophys. Res., 114, D08303, doi:10.1029/2008jd010621, 2009.

Pfister, G. G., Emmons, L. K., Edwards, D. P., Arellano, A., G Sachse, and Campos, T.: Variability of springtime transpacific pollution transport during 2000–2006: the INTEX-B mission in the context of previous years, Atmos. Chem. Phys., 10, 1345–1359, doi:10.5194/acp-10-1345-2010, 2010.

Pope, C. A. and Dockery, D. W.: Health effects of fine particulate air pollution: lines that connect, J. Air Waste Manage., 56, 709–742, 2006.

Presto, A. A. and Donahue, N. M.: Investigation of alpha-pinene plus ozone secondary organic aerosol formation at low total aerosol mass, Environ. Sci. Technol., 40, 3536–3543, doi:10.1021/es052203z, 2006.

Rasch, P. J., Mahowald, N. M., and Eaton, B. E.: Representations of transport, convection, and the hydrologic cycle in chemical transport models: Implications for the modeling of short-lived and soluble species, J. Geophys. Res., 102, 28127–28138, doi:10.1029/97jd02087, 1997.

Robinson, N. H., Hamilton, J. F., Allan, J. D., Langford, B., Oram, D. E., Chen, Q., Docherty, K., Farmer, D. K., Jimenez, J. L., Ward, M. W., Hewitt, C. N., Barley, M. H., Jenkin, M. E., Rickard, A. R., Martin, S. T., McFiggans, G., and Coe, H.: Evidence for a significant proportion of Secondary Organic Aerosol from isoprene above a maritime tropical forest, Atmos. Chem. Phys., 11, 1039–1050, doi:10.5194/acp-11-1039-2011, 2011.

GMDD

5, 4187–4232, 2012

Russell, L. M.: Aerosol organic-mass-to-organic-carbon ratio measurements, Environ. Sci. Technol., 37, 2982–2987, doi:10.1021/es026123w, 2003.

Schwartz, J.: The effects of particulate air pollution on daily deaths: a multi-city case crossover analysis, Occup. Environ. Med., 61, 956–961, doi:10.1136/oem.2003.008250, 2004.

Simpson, D., Yttri, K. E., Klimont, Z., Kupiainen, K., Caseiro, A., Gelencser, A., Pio, C., Puxbaum, H., and Legrand, M.: Modeling carbonaceous aerosol over Europe: analysis of the CARBOSOL and EMEP EC/OC campaigns, J. Geophys. Res., 112, D23S14, doi:10.1029/2006jd008158, 2007.

Slowik, J. G., Stroud, C., Bottenheim, J. W., Brickell, P. C., Chang, R. Y.-W., Liggio, J., Makar, P. A., Martin, R. V., Moran, M. D., Shantz, N. C., Sjostedt, S. J., van Donkelaar, A., Vlasenko, A., Wiebe, H. A., Xia, A. G., Zhang, J., Leaitch, W. R., and Abbatt, J. P. D.: Characterization of a large biogenic secondary organic aerosol event from eastern Canadian forests, Atmos. Chem. Phys., 10, 2825–2845, doi:10.5194/acp-10-2825-2010, 2010.

Spracklen, D. V., Jimenez, J. L., Carslaw, K. S., Worsnop, D. R., Evans, M. J., Mann, G. W., Zhang, Q., Canagaratna, M. R., Allan, J., Coe, H., McFiggans, G., Rap, A., and Forster, P.: Aerosol mass spectrometer constraint on the global secondary organic aerosol budget, Atmos. Chem. Phys., 11, 12109–12136, doi:10.5194/acp-11-12109-2011, 2011.

Tang, Y., Lee, P., Tsidulko, M., Huang, H.-C., McQueen, J. T., DiMego, G. J., Emmons, L. K., Pierce, R. B., Thompson, A. M., Lin, H.-M., Kang, D., Tong, D., Yu, S., Mathur, R., Pleim, J. E., Otte, T. L., Pouliot, G., Young, J. O., Schere, K. L., Davidson, P. M., and Stajner, I.: The impact of chemical lateral boundary conditions on CMAQ predictions of tropospheric ozone over the continental United States, Environ. Fluid Mech., 9, 43–58, doi:10.1007/s10652-008-9092-5, 2009.

Tsigaridis, K. and Kanakidou, M.: Secondary organic aerosol importance in the future atmosphere, Atmos. Environ., 41, 4682–4692, doi:10.1016/j.atmosenv.2007.03.045, 2007.

Tsimpidi, A. P., Karydis, V. A., Zavala, M., Lei, W., Molina, L., Ulbrich, I. M., Jimenez, J. L., and Pandis, S. N.: Evaluation of the volatility basis-set approach for the simulation of organic aerosol formation in the Mexico City metropolitan area, Atmos. Chem. Phys., 10, 525–546, doi:10.5194/acp-10-525-2010, 2010.

Valorso, R., Aumont, B., Camredon, M., Raventos-Duran, T., Mouchel-Vallon, C., Ng, N. L., Seinfeld, J. H., Lee-Taylor, J., and Madronich, S.: Explicit modelling of SOA formation from α-pinene photooxidation: sensitivity to vapour pressure estimation, Atmos. Chem. Phys., 11, 6895–6910, doi:10.5194/acp-11-6895-2011, 2011.

GMDD

5, 4187–4232, 2012

van der Werf, G. R., Randerson, J. T., Giglio, L., Collatz, G. J., Kasibhatla, P. S., and Arellano Jr., A. F.: Interannual variability in global biomass burning emissions from 1997 to 2004, Atmos. Chem. Phys., 6, 3423–3441, doi:10.5194/acp-6-3423-2006, 2006.

Volkamer, R., Jimenez, J. L., San Martini, F., Dzepina, K., Zhang, Q., Salcedo, D., Molina, L. T., Worsnop, D. R., and Molina, M. J.: Secondary organic aerosol formation from anthropogenic air pollution: rapid and higher than expected, Geophys. Res. Lett., 33, L17811, doi:10.1029/2006gl026899, 2006.

Wespes, C., Emmons, L., Edwards, D. P., Hannigan, J., Hurtmans, D., Saunois, M., Coheur, P.-F., Clerbaux, C., Coffey, M. T., Batchelor, R. L., Lindenmaier, R., Strong, K., Weinheimer, A. J., Nowak, J. B., Ryerson, T. B., Crounse, J. D., and Wennberg, P. O.: Analysis of ozone and nitric acid in spring and summer Arctic pollution using aircraft, ground-based, satellite observations and MOZART-4 model: source attribution and partitioning, Atmos. Chem. Phys., 12, 237–259, doi:10.5194/acp-12-237-2012, 2012.

Zhang, Q., Canagaratna, M. R., Jayne, J. T., Worsnop, D. R., and Jimenez, J. L.: Time- and size-resolved chemical composition of submicron particles in Pittsburgh: implications for aerosol sources and processes, J. Geophys. Res., 110, D07S12, doi:10.1029/2004jd004649, 2005.

GMDD
5, 4187–4232, 2012

Table 1. Original (base-case and MZ4-v1 simulations) and newly treated (MZ4-v2) parent VOCs contributing to SOA production in MOZART-4. Model parameters are for $\rho = 1.0\,\mathrm{g\,cm^{-3}}$ and $T = 298\,\mathrm{K}$ and are based on 2p-VBS fits with the exception of NO_3 oxidation of monoterpenes and OH oxidation of isoprene, which are based on Chung and Seinfeld (2002) and Henze and Seinfeld (2006), respectively.

MOZART-4 Parent VOC	SPRC 99	Oxidant	α_1	K_{om1}	α_2	K_{om2}
$C_{10}H_{16}$ (lumped monoterpenes as α-pinene)	TERP	O_3/OH	0.289	0.008	0.086	0.205
$C_{10}H_{16}$ (lumped monoterpenes as α-pinene)	TERP	NO_3	1.000	0.016	0.000	0.000
TOLUENE (C_7H_8: lumped aromatics)	ARO1	OH	0.325	0.008	0.124	0.146
BIGALK (C_5H_{12}: lumped alkanes with C > 3)	ALK3 + ALK4 + ALK5	OH	0.100	0.150	0.047	0.080
Added in MZ4-v2						
ISOP (C_5H_8: isoprene)	ISOPRENE	OH	0.178	0.011	0.022	2.106
BIGENE (C_4H_8: lumped alkenes with C > 3)	OLE2	OH	0.144	0.006	0.022	0.185
C_3H_6 (propene)	OLE1	OH	0.078	0.005	0.006	0.167

GMDD
5, 4187–4232, 2012

Table 2. Global surface emissions of POA and SOA precursors from anthropogenic and biogenic sources.

Type/Species	Emissions (Tg yr^{-1})
POA (hydrophobic + hydrophilic)*	63
Anthropogenic	
TOLUENE (C_7H_8: lumped aromatics)	33
BIGALK (C_5H_{12}: lumped alkanes with C > 3)	77
BIGENE (C_4H_8: lumped alkenes with C > 3)	9
C_3H_6 (propene)	6
Biogenic	
$C_{10}H_{16}$ (lumped monoterpenes as α-pinene)	89
ISOP (C_5H_8: isoprene)	462

* A multiplication factor of 1.4 (Griffin et al., 1999) was used to convert primary organic carbon (POC) to primary organic aerosol (POA) mass.

GMDD
5, 4187–4232, 2012

Table 3. Regionally-averaged annual SOA concentrations at the surface for the year 2006.

Region	Annual average ($\pm 1\sigma$) SOA ($\mu g\,m^{-3}$) at the surface		
	Base-case	Updated (MZ4-v1)	Updated (MZ4-v2)
Canada (50–70° N, 125–60° W)	0.07 ± 0.03	0.08 ± 0.04	0.14 ± 0.09
USA (25–50° N, 125–60° W)	0.09 ± 0.05	0.14 ± 0.10	0.37 ± 0.27
Europe (35–70° N, 10° W–45° E)	0.12 ± 0.07	0.25 ± 0.17	0.47 ± 0.29
North Asia (45–70° N, 60–150° E)	0.06 ± 0.05	0.08 ± 0.08	0.17 ± 0.18
Southeast Asia (10–45° N, 60–125° E)	0.10 ± 0.11	0.18 ± 0.18	0.56 ± 0.66
Indonesia (10° S10° N, 90–150° E)	0.31 ± 0.38	0.36 ± 0.44	1.57 ± 1.88
North Africa (Eq–30° N, 20° W–55° E)	0.07 ± 0.11	0.09 ± 0.12	0.36 ± 0.50
South Africa (40° S–Eq, 0–55° E)	0.08 ± 0.09	0.09 ± 0.11	0.45 ± 0.37
South America (30° S–Eq, 90–30° W)	0.36 ± 0.50	0.39 ± 0.52	1.00 ± 1.04
Australia (45–10° S, 110–160° E)	0.06 ± 0.07	0.07 ± 0.08	0.52 ± 0.34

GMDD
5, 4187–4232, 2012

Table 4. Regionally-averaged base-case annual AOD and its increases due to additional SOA predicted by the updated version of MOZART-4 (MZ4-v2). Also, shown in parenthesis, is the range of monthly average increase in total AOD due to SOA.

	Base-case		MZ4-v2
Region	Total AOD	POA and SOA contributions to Total AOD (%)	Increase in total AOD attributed to SOA (%)
Canada (50–70° N, 125–60° W)	0.23	7	0.9 (0.1–2.1)
USA (25–50° N, 125–60° W)	0.32	6	1.2 (0.3–3)
Europe (35–70° N, 10° W–45° E)	0.60	5	0.6 (0.1–1.8)
North Asia (45–70° N, 60–150° E)	0.38	7	0.6 (0.1–1.4)
Southeast Asia (10–45° N, 60–125° E)	0.62	5	1.8 (1.0–2.4)
Indonesia (10° S10° N, 90–150° E)	0.18	21	4.4 (1.1–15.7)
North Africa (Eq–30° N, 20° W–55° E)	0.73	3	2.9 (1.3–5.3)
South Africa (40° S–Eq, 0–55° E)	0.14	19	2.8 (1.3–8.2)
South America (30° S–Eq, 90–30° W)	0.15	14	6.2 (2.6–13.3)
Australia (45–10° S, 110–160° E)	0.14	9	7.7 (3.6–30.4)
North Pacific Ocean (Eq–60° N, 135° E–100° W)	0.20	6	2.3 (1.2–3.2)
North Atlantic Ocean (Eq–60° N, 0–80° W)	0.39	3	2.9 (1.5–3.4)
South Pacific Ocean (45° S–Eq, 150° E–80° W)	0.08	6	8.2 (4.5–17.6)
South Atlantic Ocean (45° S–Eq, 60° W–15° E)	0.13	13	4.1 (2.2–8.9)
Indian Ocean (45° S–30° N, 30–150° E)	0.24	7	4.1 (2.2–6.9)

GMDD
5, 4187–4232, 2012

Table 5. Global SOA budget estimates.

Model versions	Removal (Tg yr^{-1}) Dry	Removal (Tg yr^{-1}) Wet	Production (Tg yr^{-1})	Lifetime (days)	Burden (Tg)
Base-case	1.1	4.7	5.8	13.6	0.22
Updated – MZ4-v1	1.4	5.2	6.6	13.1	0.24
Updated – MZ4-v2	4.7	14.4	19.1	11.2	0.59

GMDD
5, 4187–4232, 2012

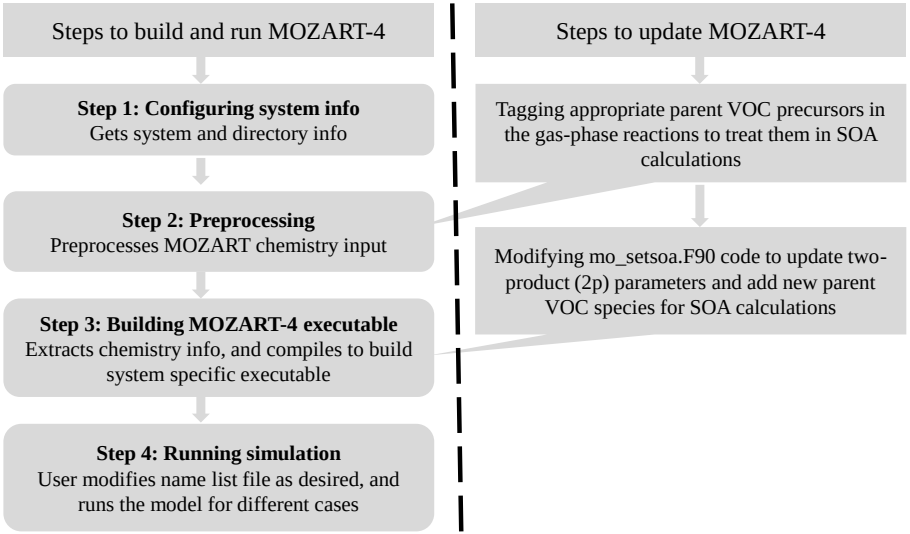

Fig. 1. Schematic showing steps to build and run MOZART-4 executable, and updates to SOA module in the global chemical transport modeling system.

GMDD
5, 4187–4232, 2012

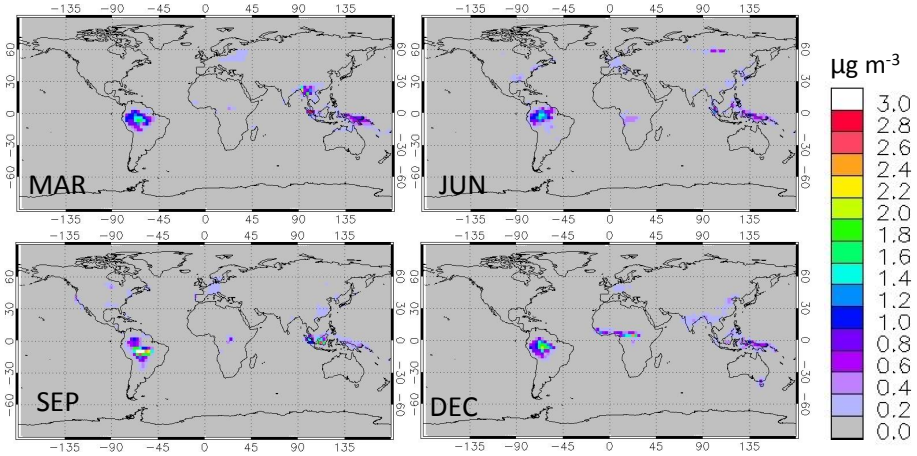

Fig. 2. Global distributions of monthly average SOA concentrations (µg m^{-3}) at the surface predicted in the base-case MOZART-4 runs for March, June, September and December of 2006. Note that the concentration, production and burden of SOA actually represent the mass of C (µg C m^{-3}) in this work.

GMDD
5, 4187–4232, 2012

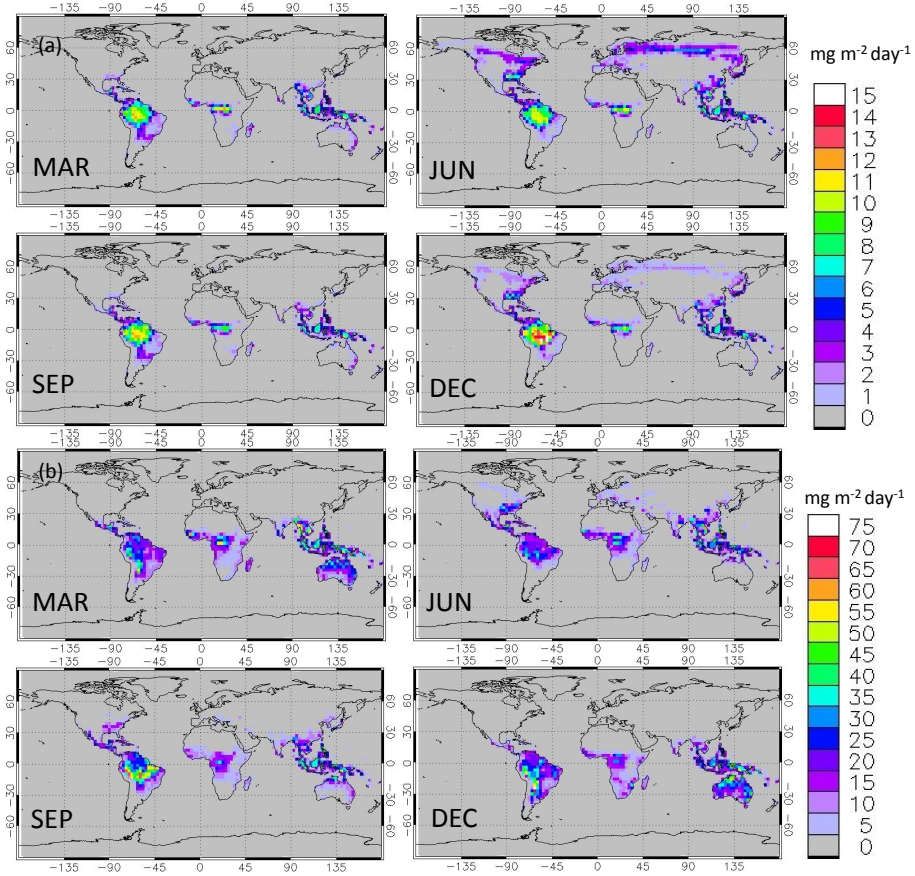

Fig. 3. Global distributions of monthly average emissions rates (mg m^{-2} day^{-1}) for **(a)** summed monoterpenes ($C_{10}H_{16}$), and **(b)** isoprene (C_5H_8) at the surface. Examples are shown for representative months in different seasons of the year. Note that emissions rates are based on the mass of C (mg C m^{-2} day^{-1}) rather than the mass of individual VOC in this work.

GMDD
5, 4187–4232, 2012

Improving the representation of SOA in MOZART-4

A. Mahmud and K. C. Barsanti

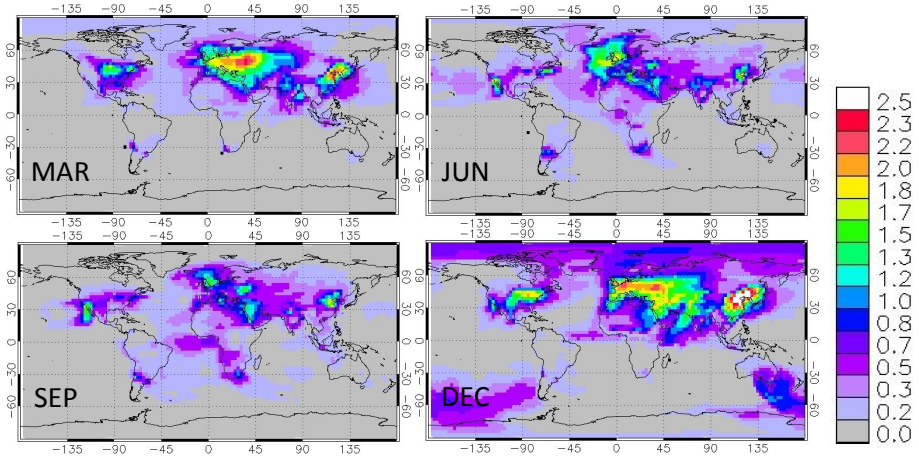

Fig. 4. Fractional change in simulated surface SOA concentrations due to two-product (2p) parameter updates (MZ4-v1) relative to the base-case.

GMDD
5, 4187–4232, 2012

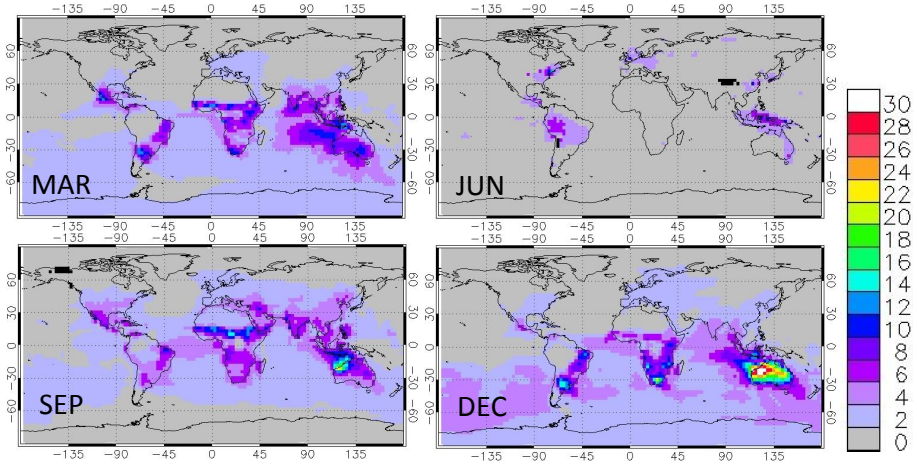

Fig. 5. Fractional change in simulated surface SOA concentrations due to 2p parameter updates and consideration of additional SOA precursors (MZ4-v2) relative to the base-case.

GMDD
5, 4187–4232, 2012

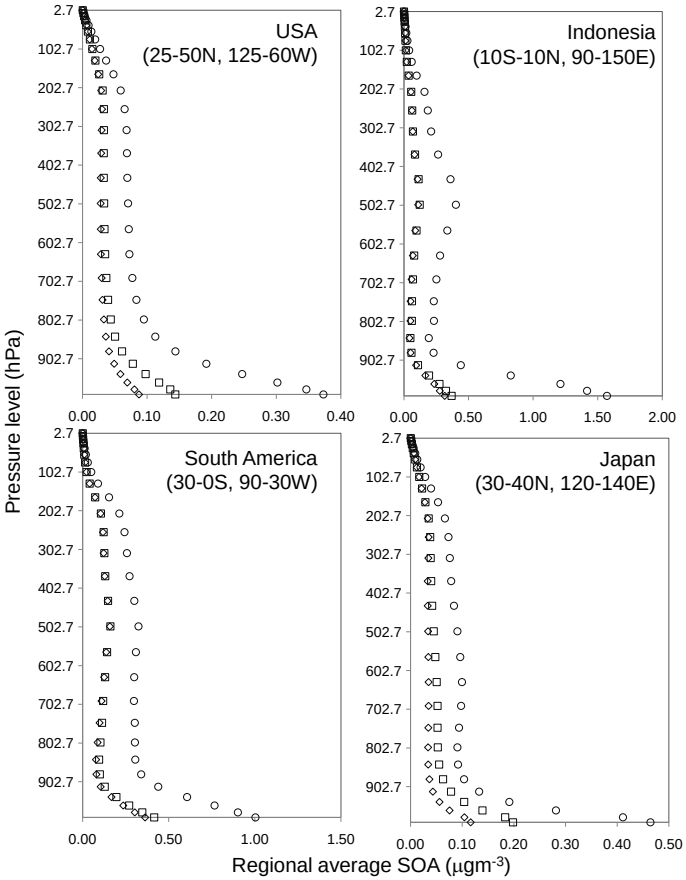

Fig. 6. Vertical distributions of regionally-averaged annual SOA concentrations (μg m^{-3}). Simulated SOA concentrations for the base-case are represented by open diamonds; open squares represent updated version, MZ4-v1 (updated 2p parameters), and open circles represent updated version, MZ4-v2 (updated 2p parameters and additional parent VOCs).

GMDD
5, 4187–4232, 2012

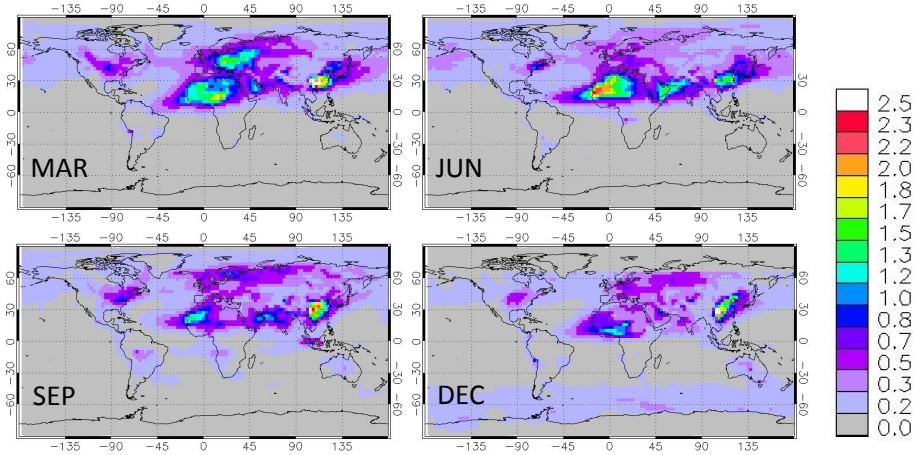

Fig. 7. Global distributions of monthly average total aerosol optical depth (AOD) for the base-case MOZART-4 simulations.

GMDD
5, 4187–4232, 2012

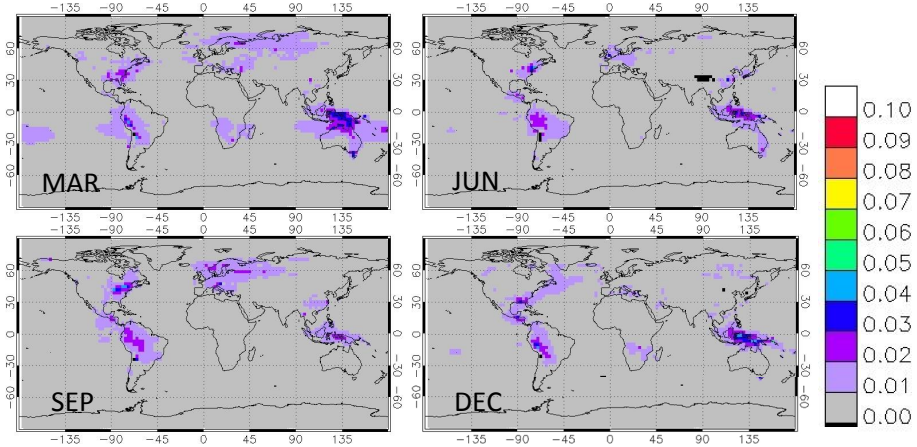

Fig. 8. Fractional increase in total AOD at the surface from the base-case MOZART-4 simulations due to updates to 2p parameters and treatment of additional SOA precursor species (MZ4-v2).

GMDD
5, 4187–4232, 2012